



SOME NEW MODELS OF CHARGED DARK ENERGY STARS IN CONFORMAL SYMMETRY

MANUEL MALAVER DE LA F.^{1,2,3} y MARIA ESCULPI³

Department of Basic Sciences, Maritime University of the Caribbean, Catia la Mar, Venezuela¹

Institute of Scholars, Muddhinapalya Bengaluru-560091, Karnataka, India²

Department of Applied Physics, Engineering Faculty, Central University of Venezuela³

{mmf.umc, mariaesculpiw}@gmail.com

Recibido: 29/07/2025, Revisado: 07/08/2025, Aceptado: 07/08/2025

Abstract

We obtained some stellar configurations that represent new models of dark energy stars in presence of a conformal Killing vector with the linear equation of state $p_r = \omega\rho$, where ω is the dark energy parameter, p_r is the radial pressure and ρ is the energy density. By combining the linear equation of state with the Einstein-Maxwell field equations, an equation for electric field is obtained. The generated solution well behaved in the stellar interior but it is important to mention that the denomination of dark energy is applied to fluids which violate the strong energy condition and the causality. Since multiple independent observations suggest that the universe is experiencing accelerated expansion, which can be explained by the presence of undetected dark energy. The models are consistent with the upper limit on the mass of compact stars for 4U1700-377, PSR J1600-3053, PSR J1759+5036 and PSR J1748-2021B.

Keywords: Dark energy, Conformal Killing vector, Linear equation of state, Strong Energy, Causality.

Nuevos modelos de estrellas cargadas de energía oscura en simetría conforme

Resumen

Hemos obtenido algunas configuraciones estelares que representan nuevos modelos de estrellas de energía oscura en presencia de un vector conforme de Killing con la ecuación lineal de estado, donde ω es el parámetro de energía oscura, p_r es la presión radial y ρ es la densidad de energía. Combinando la ecuación lineal de estado con las ecuaciones de campo de Einstein-Maxwell, se obtiene una ecuación para el campo eléctrico. La solución generada se comporta bien en el interior estelar pero es importante mencionar que la denominación de energía oscura se aplica a fluidos que violan la condición de energía fuerte y la causalidad. Varias observaciones independientes sugieren que el universo está experimentando una expansión acelerada, lo que puede explicarse por la presencia de energía oscura no detectada. Los modelos son consistentes con el límite superior de la masa de las estrellas compactas 4U1700-377, PSR J1600-3053, PSR J1759+5036 y PSR J1748-2021B.

Palabras clave: Energía oscura, Vector conforme de Killing, Ecuación lineal de estado, Energía fuerte, Causalidad.

1. Introduction

Most galaxies have gas and dust clouds with a non-uniform matter distribution, which is where stars are produced. White dwarfs and neutron stars that develop at the end of their stellar evolution are typically referred to as "compact objects" in astronomy (Bicak, 2006; Kuhfitting, 2011). Strong gravitational fields and high densities are characteristics of compact objects. In order to investigate powerful gravitational forces, Albert Einstein developed the general theory of relativity (GR) in 1915. The hypothesis is regarded as the fundamental framework for studies in star astrophysics. The structure and behavior of celestial objects can be studied and understood with the use of the Einstein field equations (EFEs). Schwarzschild came up with the first solution to the EFEs in 1916 (Schwarzschild, 1916). Since then, a number of scholars have examined these equations in various ways, and a number of astrophysical models have been developed to offer a thorough explanation of the distribution of mass within star bodies (Chandrasekhar, 1931; Oppenheimer, 1939; Tolman, 1939). By extending Newton's law of universal gravitation and generalizing special relativity, the GR theory describes gravity as a geometric characteristic of space and time (Lobo, 2005; Sushkov, 2005). Currently, several authors (Bibi *et al.*, 2016; Chan *et al.*, 2009; Dayanandan & Smitha, 2021; Lobo, 2005; Lobo, 2006; Malaver, 2013; Malaver & Esculpi, 2013; Malaver *et al.*, 2019; Malaver & Kasmaei, 2020; Morris & Thorne, 1988; Visser, 1995) have produced some solutions to the EFEs for compact star models.

Current astronomical data as the measurements of supernovas of type Ia and microwave background radiation are the most direct evidences of the accelerated expansion of the universe (Lobo, 2006). The explanation for this cosmological behavior in the framework of general relativity requires assumption that a considerable part of the Universe consists of a hypothetical dark energy with a negative pressure component (Sushkov, 2005; Lobo, 2005; Lobo, 2006), which is a cosmic fluid parameterized by $p_r = \omega\rho$ with $-1 \leq \omega \leq -1/3$ where p is the spatially homogeneous pressure and ρ the dark energy density (Bibi, *et al.*, 2016; Lobo, 2006; Malaver, 2013). According to Chan *et al.*, (2009) the denomination of dark energy is applied to fluids which violate only the strong energy condition (SEC) given by $\rho + p_r + 2p_t \geq 0$ where ρ is the energy density, p_t and p_r are the radial pressure and tangential pressure, respectively.

Studying the characteristics and behavior of compact stars has also benefited from the application of conformal symmetry. These potentials are subject to particular constraints when the conformal Killing vector is imposed on the space-time manifold, which makes the process of solving the field equations easier. This method produces a number of models, including (Manjonjo *et al.*, 2017; Rahaman *et al.*, 2010). Equations of state and conformal symmetry with single-layered stars were investigated by some few authors in the past. A relativistic compact star model with a linear equation of state and a conformal Killing vector in the presence of charge was produced by Jape *et al.*, (2023). Christopher *et al.*, (2024) used a quadratic equation of state in

addition to the conformal Killing vector to examine the properties of a relativistic charged compact star.

In this work, we combine a linear equation of state with a dark energy parameter and the conformal Killing vector (CKV) to examine the physics and behavior of a charged dark energy star. In Sec. 2, the Einstein-Maxwell field equations used to generate the model are presented. We give a detailed description of conformal Killing Vector in Sec. 3. By choosing of a gravitational potential that allow the field equations to be solved, we construct new models for charged anisotropic matter in section 4. In Section 5, the physical acceptability requirements are discussed. The validity and physical properties of these new solutions are examined in Section 6. The concluding remarks are provided in Section 7.

2. Einstein Field Equations

We consider a spherically symmetric, static and homogeneous and anisotropic spacetime in Schwarzschild coordinates given by

$$ds^2 = -e^{2\nu(r)} dt^2 + e^{2\lambda(r)} dr^2 + r^2(d\theta^2 + \sin^2\theta d\phi^2) \quad (1)$$

where $\nu(r)$ and $\lambda(r)$ are two arbitrary functions.

The Einstein field equations for the charged anisotropic matter are given by

$$\frac{1}{r^2} \left(1 - e^{-2\lambda} \right) + \frac{2\lambda'}{r} e^{-2\lambda} = \rho + \frac{1}{2} E^2 \quad (2)$$

$$-\frac{1}{r^2} \left(1 - e^{-2\lambda} \right) + \frac{2\nu'}{r} e^{-2\lambda} = p_r - \frac{1}{2} E^2 \quad (3)$$

$$e^{-2\lambda} \left(\nu'' + \nu'^2 + \frac{\nu'}{r} - \nu'\lambda' - \frac{\lambda'}{r} \right) = p_t + \frac{1}{2} E^2 \quad (4)$$

$$\sigma = \frac{1}{r^2} e^{-\lambda} (r^2 E)' \quad (5)$$

where ρ is the energy density, p_r is the radial pressure, E is electric field intensity and

p_t is the tangential pressure, respectively.

Using the transformations, $x = cr^2$, $Z(x) = e^{-2\lambda(r)}$ and $A_*^2 y^2(x) = e^{2\nu(r)}$ with arbitrary constants A_* and $c > 0$ (Durgapal & Bannerji, 1983), the metric (1) take the form

$$ds^2 = -A^2 y^2(x) dt^2 + \frac{dx^2}{4Z(x)Cx} + \frac{x}{C} (d\theta^2 + \sin^2\theta d\phi^2)$$

and the Einstein field equations can be written as

$$\frac{1-Z}{x} - 2\dot{Z} = \frac{\rho}{c} + \frac{E^2}{2c} \quad (6)$$

$$4Z \frac{\dot{y}}{y} - \frac{1-Z}{x} = \frac{p_r}{c} - \frac{E^2}{2c} \quad (7)$$

$$4xZ \frac{\ddot{y}}{y} + (4Z + 2x\dot{Z}) \frac{\dot{y}}{y} + \dot{Z} = \frac{p_t}{c} + \frac{E^2}{2c} \quad (8)$$

$$p_t = p_r + \Delta \quad (9)$$

$$\frac{\Delta}{c} = 4xZ \frac{\ddot{y}}{y} + \dot{Z} \left(1 + 2x \frac{\dot{y}}{y} \right) + \frac{1-Z}{x} - \frac{E^2}{c} \quad (10)$$

$$\sigma^2 = \frac{4cZ}{x} (x\dot{E} + E)^2 \quad (11)$$

σ is the charge density and dots denoting differentiation with respect to x . With the transformations of , the mass within a radius r of the sphere take the form

$$M(x) = \frac{1}{4c^{3/2}} \int_0^x \sqrt{x} \rho(x) dx \quad (12)$$

The interior metric (1) with the charged matter distribution should match the exterior spacetime described by the Reissner-Nordström metric:

$$ds^2 = - \left(1 - \frac{2M}{r} + \frac{Q^2}{r^2} \right) dt^2 + \left(1 - \frac{2M}{r} + \frac{Q^2}{r^2} \right)^{-1} dr^2 + r^2 (d\theta^2 + \sin^2 \theta d\varphi^2) \quad (13)$$

where the total mass and the total charge of the star are denoted by M and q^2 , respectively. The junction conditions at the stellar surface are obtained by matching the first and the second fundamental forms for the interior metric (1) and the exterior metric (13).

In this paper, we assume the following equation of state

$$p_r = \omega \rho \quad (14)$$

where ω is the dark energy parameter.

3. Conformal symmetry

We examine the manifold of spacetime that admits conformal symmetry. The system's EFEs (2-4) are made simpler by the conformal Killing vector's imposition (CKV). The application of CKV results in new exact solutions for the core-envelope model in conjunction with the equation of state. The conformal Killing vector is defined as (Herrera *et al.*, 1984)

$$LX(r,t)g_{ab} = 2\phi(r,t)g_{ab} \quad (15)$$

where L is the Lie derivate operator, $X(r,t)$ stands for vector field, g_{ij} is the metric tensor and $\phi(r,t)$ is a conformal factor. With symmetry assumption, the conformal Killing vector and the conformal factor in (15) are given by

$$X = \alpha(t,r) \frac{\partial}{\partial t} + \beta(t,r) \frac{\partial}{\partial r} \quad (16)$$

$$\phi = \phi(r, t)$$

(17)

We take into account the related Weyl tensor integrability requirement (Weyl, 1918) in order to solve equation (15)

$$LX(r, t)C^i_{jkl} = 0$$

(18)

where C^i_{jkl} are the Weyl tensor components. With the eq. (18), eq. (15) can be expressed as

$$\nu'' + (\nu')^2 - \nu'\lambda' - \frac{\nu' - \lambda'}{r} + \frac{1}{r^2} = \frac{e^{2\lambda}(1+k)}{r^2}$$

(19)

where k represents a real constant.

With the transformations, $x = cr^2$, $Z(x) = e^{-2\lambda(r)}$ and $A_*^2 y^2(x) = e^{2\nu(r)}$ suggested for Durgapal & Bannerji (1983) and the condition $k = 2(n-1)$ we obtain

$$y(x) = \begin{cases} A\sqrt{x} \exp\left(\frac{1}{2}\sqrt{2n-1} \int \frac{dx}{x\sqrt{Z}}\right) + B\sqrt{x} \exp\left(-\frac{1}{2}\sqrt{2n-1} \int \frac{dx}{x\sqrt{Z}}\right) \rightarrow n > 1/2 \\ A\frac{\sqrt{x}}{2} \int \frac{dx}{x\sqrt{Z}} + B\sqrt{x} \rightarrow n = 1/2 \\ A\sqrt{x} \exp\left(\frac{1}{2}\sqrt{-(2n-1)} \int \frac{dx}{x\sqrt{Z}}\right) + B\sqrt{x} \exp\left(-\frac{1}{2}\sqrt{-(2n-1)} \int \frac{dx}{x\sqrt{Z}}\right) \rightarrow n < 1/2 \end{cases}$$

(20)

where A and B are constant parameters and $n=1$ represents a conformally flat spacetime.

4. A new class of models

In this section, we found the novel solution for the charged dark energy star that admits a linear equation of state and conformal symmetry. Substituting eq. (14) in the equations (6-7) for the electric field intensity we can obtain

$$\frac{E^2}{2C} = \left(\frac{1-Z}{x}\right) - 2\dot{Z} - \frac{1}{\omega+1} \left(4Z \frac{\dot{y}}{y} - 2\dot{Z}\right)$$

(21)

where ω is the dark energy parameter and Z is the chosen metric potential that can be written as

$$Z(x) = \left(\frac{1-ax}{1+ax}\right)^2$$

(22)

With the conformal condition (20) and eq. (22) and considering case $n=1$, the second gravitational potential is written as

$$y(x) = \frac{Ax}{ax-1} + B(ax-1)$$

(23)

With the equations (21) and (22) and substituting eq. (23) in (6), we obtain for the energy density

$$\rho = \frac{C}{\omega+1} \left(\frac{4(1-ax)^2}{(1+ax)^2(ax-1)} \left[\frac{-A + aB(ax-1)^2}{[Ax + B(ax-1)^2]} \right] + \frac{8a(1-ax)}{(1+ax)^3} \right)$$

(24)

and for the radial pressure

$$P_r = \frac{\omega C}{\omega + 1} \left(\frac{4(1-ax)^2}{(1+ax)^2(ax-1)} \left[\frac{-A + aB(ax-1)^2}{Ax + B(ax-1)^2} \right] + \frac{8a(1-ax)}{(1+ax)^3} \right) \quad (25)$$

Using the equations (22) and (23) and their derivatives, the electric field intensity can be written as

$$\frac{E^2}{2C} = \frac{4a(3-ax)}{(1+ax)^3} - \frac{1}{\omega + 1} \left[\frac{-4A(ax-1) + 4aB(ax-1)^3}{Ax(ax+1)^2 + B(a^2x^2-1)^2} + \frac{8a(1-ax)}{(1+ax)^3} \right] \quad (26)$$

With (22) and (26) the charge density in (11) take the form

$$\sigma^2 = \frac{4C(1-ax)^2}{x(1+ax)^2} \left[\frac{x}{2} \left[\frac{8aC(3-ax)}{(1+ax)^3} - \frac{2CJ(x)}{\omega + 1} \right]^{-1/2} + \left[\frac{8aC(3-ax)}{(1+ax)^3} - \frac{2CJ(x)}{\omega + 1} \right]^{1/2} \right] \quad (27)$$

Where for convenience we taken

$$J(x) = \frac{-4A(ax-1) + 4aB(ax-1)^3}{Ax(ax+1)^2 + B(a^2x^2-1)^2} + \frac{8a(1-ax)}{(1+ax)^3} \quad \text{and}$$

$$K(x) = \frac{\left[\begin{aligned} &[-4aA + 12a^2B(ax-1)^2][Ax(ax+1)^2 + B(a^2x^2-1)] \\ &- [-4A(ax-1) + 4aB(ax-1)^3] \left\{ \begin{aligned} &A[(ax+1)^2 + 2ax(ax+1)] \\ &+ 4Bxa^2(a^2x^2-1) \end{aligned} \right\} \end{aligned} \right]}{[Ax(ax+1)^2 + B(a^2x^2-1)^2]^2} \quad (30)$$

By comparison of line elements (1) and (13) and considering $E|_{r=R} = Q/R^2$ we obtained for the mass of the star

$$M(x) = \frac{1}{2} \sqrt{\frac{x}{C}} \left[\begin{aligned} &1 - \frac{(1-ax)^2}{(1+ax)^2} + \frac{8ax(3-ax)}{(1+ax)^3} \\ &- \frac{2x}{\omega + 1} \left\{ \frac{4(1-ax)^2}{(1+ax)^2} \left[\frac{A}{(ax-1)^2} + aB \right] + \frac{8a(1-ax)}{(1+ax)^3} \right\} \end{aligned} \right] \quad (28)$$

With the equations (22) and (23), we have for the metric potentials

$$\left[\begin{aligned} &\frac{8aC(-10a + 2a^2x)}{(1+ax)^4} e^{2\lambda(r)} = \left(\frac{1+ax}{1-ax} \right)^2 \\ &\left(\frac{29}{2C} \left[K(x) + \frac{8a(-4a + 2a^2x)}{\omega + 1} \right] \right)^2 \\ &e^{2\nu(r)} = A_*^2 \left(\frac{Ax}{ax-1} + B(ax-1) \right)^2 \end{aligned} \right] \quad (31)$$

and the measure of anisotropy Δ can be written as

$$\Delta = \frac{8aAx(1-ax)^2}{(1+ax)^2[Ax(ax-1)^2 + B(ax-1)^4]} - \frac{4a(1-ax)}{(1+ax)^3} \left\{ 1 + 2x \left[\frac{-A + aB(ax-1)^2}{Ax(ax-1) + B(ax-1)^3} \right] \right\} + \frac{4a}{(1+ax)^2} - \frac{8a(1-ax)}{(1+ax)^3} + \frac{2}{\omega + 1} \left[\frac{-4A(ax-1) + 4aB(ax-1)^3}{Ax(ax-1)^2 + B(a^2x^2-1)^2} + \frac{8a(1-ax)}{(1+ax)^3} \right]$$

5. Conditions of Physical Acceptability

For a model to be physically acceptable, the following conditions should be satisfied (Delgaty & Lake, 1998):

- (i) The metric potentials $e^{2\lambda}$ and $e^{2\nu}$ assume finite values throughout the stellar

interior and are singularity-free at the center $r=0$.

(ii) The energy density ρ should be positive and a decreasing function inside the star.

(iii) The energy density gradient $d\rho/dr \leq 0$ for $0 \leq r \leq R$.

(iv) The anisotropy is zero at the center $r=0$, i.e. $\Delta(r=0)=0$.

(v) Any physically acceptable model must satisfy the causality condition, that is, for the radial sound speed $v_{sr}^2 = \frac{dP_r}{d\rho}$, we should

have $0 \leq v_{sr}^2 \leq 1$ but the dark energy case this condition nor is it satisfied.

(vi) The consideration of dark energy is applicable only to fluids that violate the strong energy condition

(vii) The charged interior solution should be matched with the Reissner–Nordström exterior solution, for which the metric is given by eq. (13).

The conditions (ii) and (iii) imply that the energy density must reach a maximum at the center and decrease towards the surface of the sphere.

6. Physical Features of the new Models

We now present the analysis of the physical characteristics for the new models. The metric functions $e^{2\lambda}$ and $e^{2\nu}$ have finite values and remain positive throughout the stellar interior. At the center $e^{2\lambda(0)} = 1$ and $e^{2\nu(0)} = A_*^2 B$. We show that in $r=0$ $(e^{2\lambda(r)})'_{r=0} = (e^{2\nu(r)})'_{r=0} = 0$ and this makes is possible to verify that the gravitational potentials are regular at the center. The

energy density and radial pressure are positive and well behaved within the star. Also, we have for the central density and

radial pressure $\rho(0) = \frac{4C}{\omega+1} \left(\frac{A+2aB}{B} \right)$ and

$$P_r(0) = \frac{4\omega C}{\omega+1} \left(\frac{A+2aB}{B} \right)$$

For a realistic star, it is expected that the gradient of energy density should be decreasing function of the radial coordinate r . In this model, for all $0 \leq r \leq R$, we obtain respectively:

$$\frac{d\rho}{dr} = \frac{C}{\omega+1} \left(\begin{aligned} & - \frac{16aCr(1-aCr^2)(-A+aB(aCr^2-1)^2)}{(1+aCr^2)^2(aCr^2-1)(ACr^2+B(aCr^2-1)^2)} \\ & + \frac{16a^2BCr(1-aCr^2)^2}{(1+aCr^2)^2(ACr^2+B(aCr^2-1)^2)} \\ & - \frac{16aCr(1-aCr^2)^2(-A+aB(aCr^2-1)^2)}{(aCr^2+1)^3(aCr^2-1)(ACr^2+B(aCr^2-1)^2)} \\ & - \frac{8aCr(1-aCr^2)^2(-A+aB(aCr^2-1)^2)}{(1+aCr^2)^2(aCr^2-1)^2(ACr^2+B(aCr^2-1)^2)} \\ & - \frac{4(1-aCr^2)^2(-A+aB(aCr^2-1)^2)(2ACr+4aBCr(aCr^2-1))}{(1+aCr^2)^2(aCr^2-1)(ACr^2+B(aCr^2-1)^2)^2} \\ & - \frac{16a^2Cr}{(1+aCr^2)^3} - \frac{48a^2Cr(1-aCr^2)}{(1+aCr^2)^4} \end{aligned} \right) \quad (32)$$

On the boundary $r=R$, the solution must match the Reissner–Nordström exterior space-time as:

$$ds^2 = - \left(1 - \frac{2M}{r} + \frac{Q^2}{r^2} \right) dt^2 + \left(1 - \frac{2M}{r} + \frac{Q^2}{r^2} \right)^{-1} dr^2 + r^2$$

and the continuity of e^ν and e^λ across the boundary $r=R$ is

Table 1. Values of B obtained for different dark energy parameters ω with $a = 0.001$ and $A=0.00003$

$$e^{2\nu} = e^{-2\lambda} = 1 - \frac{2M}{R} + \frac{Q^2}{R^2} \quad (33)$$

Then, for the matching conditions, we obtain

$$\frac{2M}{R} = 1 - \left(\frac{1 - aCR^2}{1 + aCR^2} \right)^2 + \frac{8aR^2(3 - aCR^2)}{(1 + aCR^2)^3} - \frac{2R^2}{\omega + 1} \left\{ \frac{4(1 - aCR^2)^2 \left[-\frac{A}{(aCR^2 - 1)^2} + aB \right]}{(1 + aCR^2)^2 \left[\frac{ACR^2}{aCR^2 - 1} + B(aCR^2 - 1) \right]} + \frac{8a(1 - aCR^2)}{(1 + aCR^2)^3} \right\} \quad (34)$$

For a physically meaningful solution, the electric field must vanish at the center of the star, i.e.,

$$\frac{E^2}{2C} = 12a - \frac{4}{\omega + 1} \left(\frac{A + aB}{B} \right) = 0 \quad (35)$$

and therefore the values of B will depend on the ω parameter of dark energy as follows

$$B = \frac{A}{(3\omega + 2)a} \quad (36)$$

In the following table shows the values of B obtained for different values of ω . For all cases $a = 0.001$ and $A = 0.00003$.

A	a	B	ω
0.00003	0.001	0.0857142857	-
0.00003	0.001	0.15	0.5
0.00003	0.001	0.27272727	0.6
0.00003	0.001	0.60	0.65

The figures 1-8 represent the plots of $\frac{E^2}{2C}$, ρ , P_r , $e^{2\nu(r)}$, $e^{2\lambda(r)}$, SEC, Δ , σ^2 , $\frac{d\rho}{dr}$, Z_s and M with the radial coordinate for different values of ω . In all the graphs we considered $C=1$.

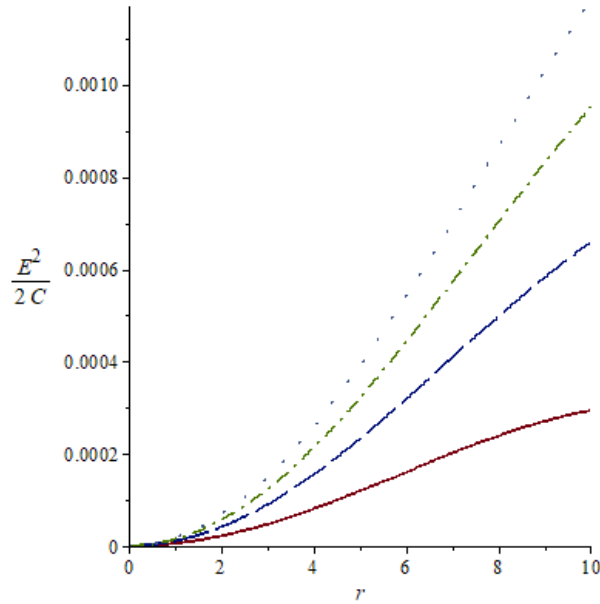


Figure 1: Electric field against the radial coordinate for $\omega = -0.55$ (solid line), $\omega = -0.60$ (long-dash line), $\omega = -0.63$ (dash-dot line) and $\omega = -0.65$ (space-dot line). For all the cases $a=0.001$, $A= 0.00003$.

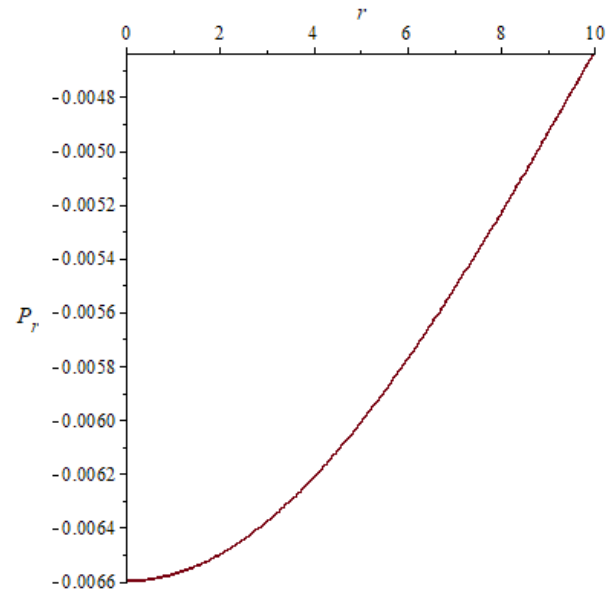


Figure 3: Radial pressure against the radial coordinate for $\omega = -0.55$ (solid line), $\omega = -0.60$ (long-dash line), $\omega = -0.63$ (dash-dot line) and $\omega = -0.65$ (space-dot line). For all the cases $a=0.001$, $A= 0.00003$.

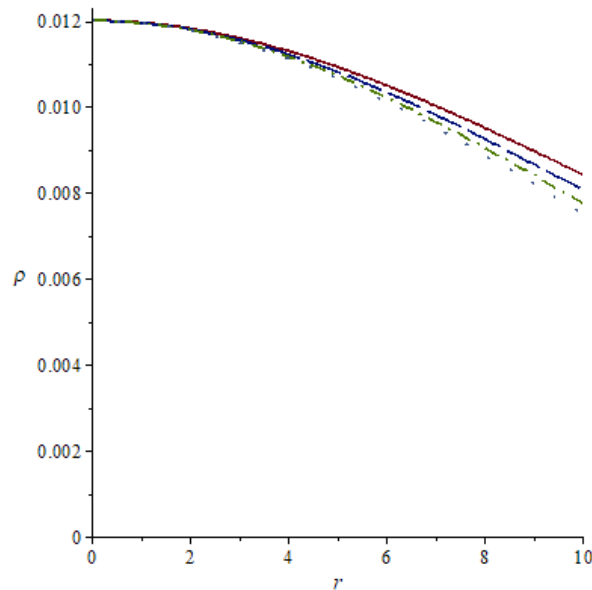


Figure 2: Energy density against the radial coordinate for $\omega = -0.55$ (solid line), $\omega = -0.60$ (long-dash line), $\omega = -0.63$ (dash-dot line) and $\omega = -0.65$ (space-dot line). For all the cases $a=0.001$, $A= 0.00003$.

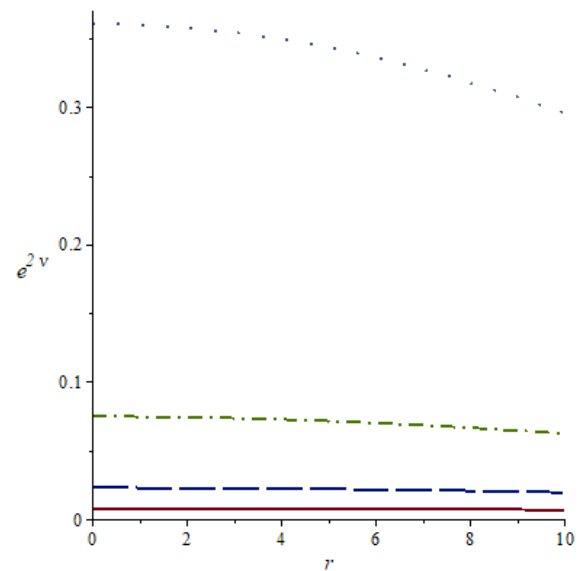


Figure 4: Metric potential e^{2v} against the radial coordinate for $\omega = -0.55$ (solid line), $\omega = -0.60$ (long-dash line), $\omega = -0.63$ (dash-dot line) and $\omega = -0.65$ (space-dot line). For all the cases $a=0.001$, $A= 0.00003$.

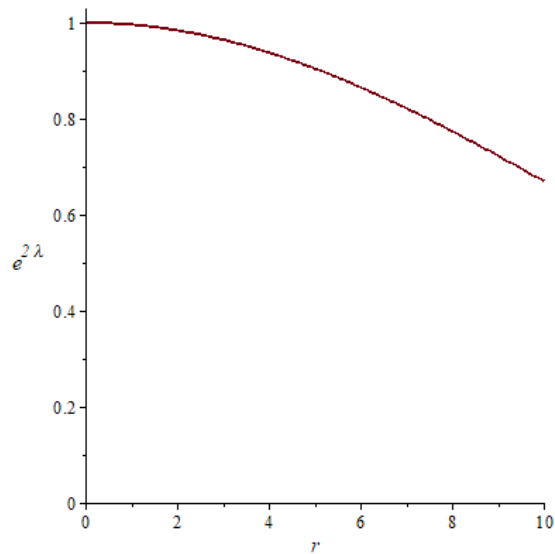


Figure 5: Metric potential $e^{2\lambda}$ against the radial coordinate for $a=0.001$

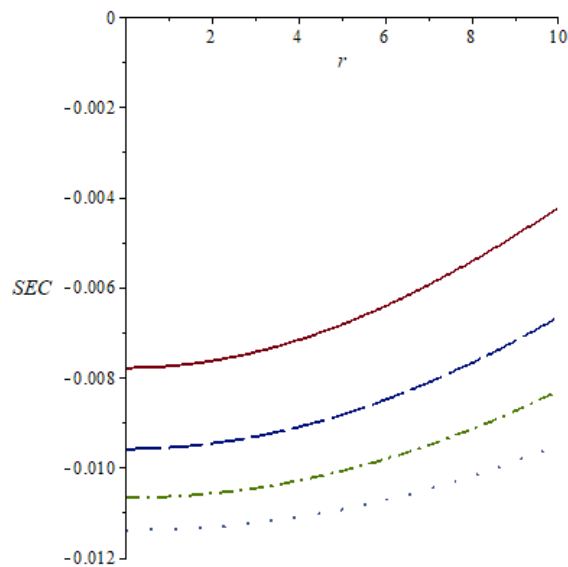


Figure 6: Strong Energy Condition (SEC) against the radial coordinate for $\omega = -0.55$ (solid line), $\omega = -0.60$ (long-dash line), $\omega = -0.63$ (dash-dot line) and $\omega = -0.65$ (space-dot line). For all the cases $a=0.001$, $A=0.00003$.

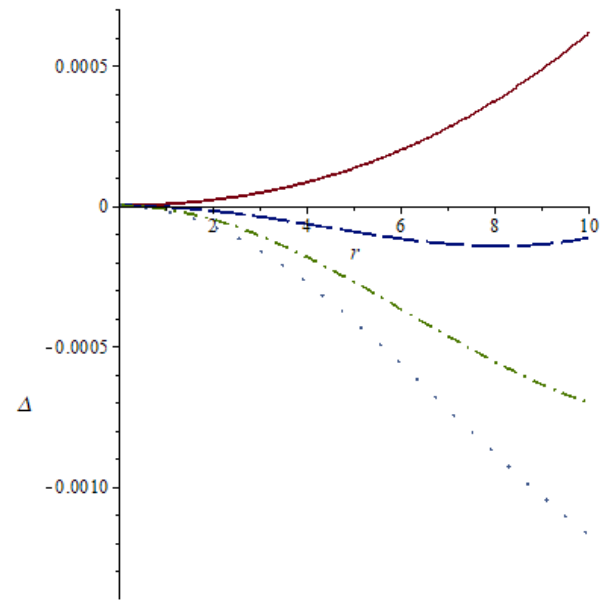


Figure 7: Anisotropy against the radial coordinate for $\omega = -0.55$ (solid line), $\omega = -0.60$ (long-dash line), $\omega = -0.63$ (dash-dot line) and $\omega = -0.65$ (space-dot line). For all the cases $a=0.001$, $A=0.00003$.

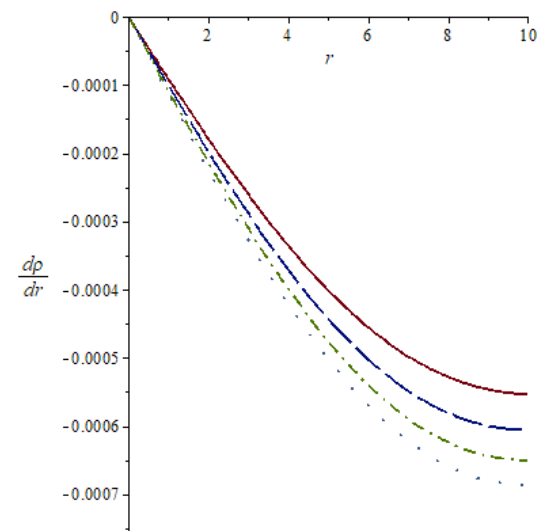


Figure 8: Energy density gradient against the radial coordinate for $\omega = -0.55$ (solid line), $\omega = -0.60$ (long-dash line), $\omega = -0.63$ (dash-dot line) and $\omega = -0.65$ (space-dot line). For all the cases $a=0.001$, $A=0.00003$.

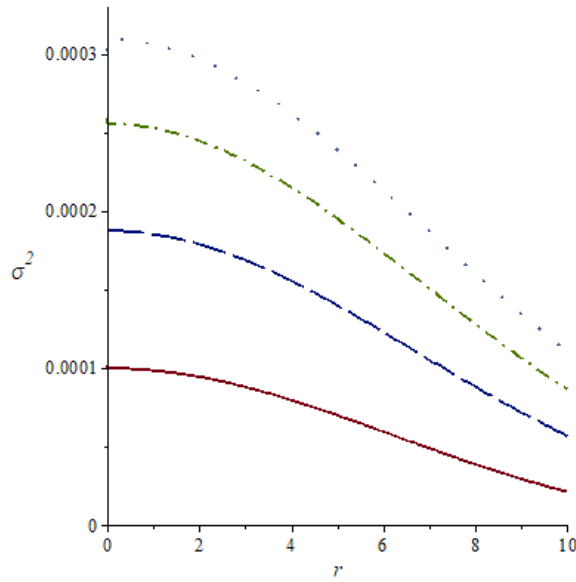


Figure 9: Charge density gradient against the radial coordinate for $\omega = -0.55$ (solid line), $\omega = -0.60$ (long-dash line), $\omega = -0.63$ (dash-dot line) and $\omega = -0.65$ (space-dot line). or all the cases $a=0.001$, $A=0.0003$.

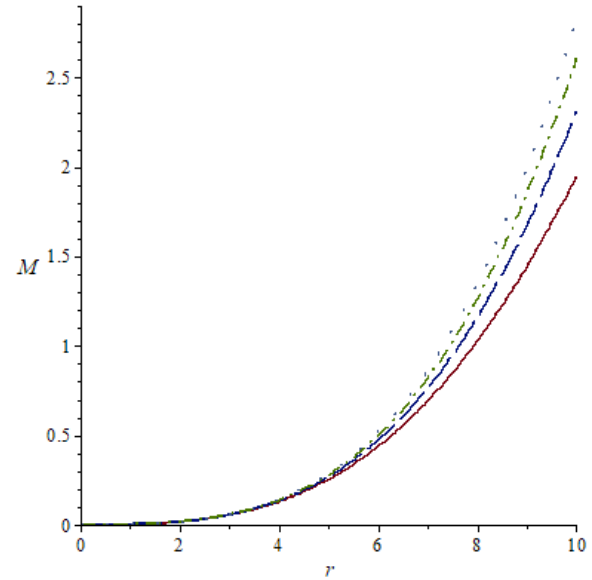


Figure 11: Mass against the radial coordinate for $\omega = -0.55$ (solid line), $\omega = -0.60$ (long-dash line), $\omega = -0.63$ (dash-dot line) and $\omega = -0.65$ (space-dot line). For all the cases $a=0.001$, $A=0.0003$.

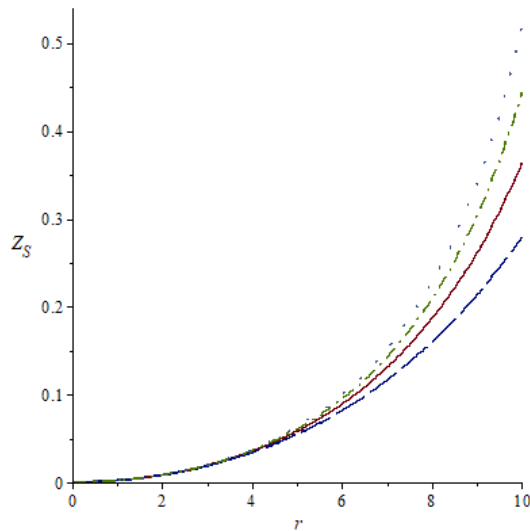


Figure 10: Surface redshift against the radial coordinate for $\omega = -0.55$ (solid line), $\omega = -0.60$ (long-dash line), $\omega = -0.63$ (dash-dot line) and $\omega = -0.65$ (space-dot line). For all the cases $a=0.001$, $A=0.0003$.

In Figure 1 the electric field intensity is a continuously growing function inside the star. The energy density remains positive, continuous and is monotonically decreasing function throughout the stellar interior as noted in Figure 2 for all the values of ω . The radial pressure is negative, not a decreasing function of the radial parameter and takes lower values when ω reduces as shown in Figure 3. Figure 4 display the behavior of the metric potential function $e^{2\nu}$ and shown that this function well behaved and remains constant for values of $\omega = -0.55; -0.60; -0.63$ but it shows a strong decrease with the radial parameter when $\omega = -0.65$. In Figure 5 the gravitational potential $e^{2\lambda}$ also is continuous and diminishes with the radial coordinate.

The Figure 6 shows that the strong energy condition is violated for all ω values considered. In Figure 7 is it noted that the anisotropy Δ grows gradually for $\omega = -0.55$ and becomes more negative as ω values diminishes and vanishes at the centre of the star. The radial variation of energy density gradient has been shown in Figure 8 and it is noted that $\frac{d\rho}{dr} < 0$ for all cases studied. In

Figure 9 the charge density is a continuously decreasing function within the stellar interior for all ω values. Figure 10 displays the surface red-shift profiles for all the values of ω and is it note that the surface redshift increases when decreases ω , reaching a maximum value of $Z_S = 0.521260114$ for $\omega = -0.65$. The mass function in Figure 11 is continuous, increasing, takes finite values, and behaves well in the interior of the star for all values of ω taken into consideration. The estimated values are comparable to the four star objects' stellar masses listed in Table 2 (Fan *et al.*, 2024; Rocha, 2023).

We note that the dark energy parameter ω modify the upper limit of the mass of compact stars. For $\omega = -0.55$, the values of a , A and B allow us to obtain a mass of $1.96M_\odot$ which can correspond to astronomic object 4U1700-377 (Rocha, 2023). With $\omega = -0.60$ the resulting mass is very similar to the pulsar J1600-3053 whose observed mass is $2.30M_\odot$ and the values of the parameters $a=0.0001$, $B=0.27272727$ for $\omega = -0.63$ generate the mass $2.62M_\odot$ that can correspond to the pulsar J1759+5036. For the case $\omega = -0.65$ we obtained a comparable mass with the

binary system J1748-2021B (Freire *et al.*, 2008).

Table 2. The approximate values of the masses for the compact stars

Compact Stars	Value s of ω	Reporte d mass $M(M_\odot)$	Calculated mass $M(M_\odot)$
4U1700-377	- 0.55	1.96	1.946305440
PSR J1600-3053	- 0.60	2.30	2.310971915
PSR J1759+5036	- 0.63	2.62	2.603956140
PSR J1748-2021B	- 0.65	2.92	2.839456340

$M_\odot =$ sun's mass

7. Conclusion

- In this work we found new class of solutions which represents a potential model for dark energy stars considering conformal symmetry.
- Relationships between metric potentials were established with the use of the conformal Killing vector.
- The gravitational potentials for the anisotropic dark energy star model generated during this work behave steadily inside the sphere.
- Anisotropy, charge density, energy density, and electric field all showed compatibility

with data in the literature and stayed within reasonable bounds for charged compact stars.

- This model not meet the strong energy criterion, but the metric potentials behave well.

- The new solutions found in this study is a realistic and physically acceptable compact star with astrophysical consequences, as demonstrated by the satisfaction of the physical constraints. We considered some known compact stars such as 4U1700-377, PSR J1600-3053, PSR J1759+5036 and PSR J1748-2021B in order to verify observational data with the model proposed in this research. We have noted that the new stellar masses generated using the new model are in a range acceptable to realistic stars.

8. References

- Bibi R, Feroze T, Siddiqui A. (2016). Solution of the Einstein-Maxwell Equations with Anisotropic Negative Pressure as a Potential Model of a Dark Energy Star. *Canadian Journal of Physics*. 94(8): 758-762.
- Bicak J. (2006). Einstein equations: exact solutions. *Encyclopaedia of Mathematical Physics* 2: 165-173.
- Chan R, da Silva MAF, Villas da Rocha J.F. (2009). On Anisotropic Dark Energy. *Mod Phys Lett A* 24: 1137-1146.
- Chandrasekhar, S. (1931). The Maximum mass of ideal white dwarfs. *Astrophys, J.* 74: 81-82.
- Christopher, J., Jape, J., Sunzu, J.M. (2024). Charged anisotropic conformal star model with a quadratic equation of state. *International Journal of Modern Physics D*. 33: 2450022
- Dayanandan B, Smitha T.T. (2021). Modelling of dark energy stars with Tolman IV gravitational potential. *Chinese Journal of Physics* 71: 683-692.
- Delgaty M.S.R, Lake, K. (1998). Physical acceptability of isolated, static, spherically symmetric, perfect fluid solutions of Einstein's equations. *Comput Phys Commun*. 115: 395
- Durgapal MC, Bannerji R.(1983). New analytical stellar model in general relativity. *Phys Rev D*. 27: 328-331.
- FanY.Z, Han M.Z., Jiang J.L., Shao D.S., Tang, S.P. (2024). Maximum gravitational mass $M_{TOV} = 2.25^{+0.08}_{-0.07} M_{\odot}$ inferred at about 3% precision with multimessenger data of neutron stars. *Phys. Rev. D* 109: 043052.
- Freire, P.C., Wolszczan, A., van der Berg, M., Hessels, J.W. (2008). A massive neutron star in the globular cluster M5. *Astrophys J*. 679: 1433.
- Herrera, L., Jimenez, J., Leal, L., Ponce de Leon, J., Esculpi, M., Galina, V. (1984). Anisotropic fluids and conformal motions in general relativity. *J.Math. Phys*, 25: 3274.
- Jape, J.W., Sunzu, J.M., Maharaj, S.D., Mkenyeleye, J.M. (2023).Charged conformal stars and equation of state. *Indian J. Phys*. 97: 1015
- Kuhfitting, P.K. (2011). Some remarks on exact wormhole solutions. *Adv Stud Theor Phys* 5: 365-367.
- Lobo, F.S.N. (2005). Stability of phantom wormholes. *Phys Rev D* 71: 124022.
- Lobo, F.S.N. (2006). Stable dark energy stars. *Class Quant Grav* 23: 1525-1541
- Lobo, F.S.N., Crawford, P. (2005). Stability analysis of dynamic thin shells. *Class Quant Grav* 22: 4869-4886.
- Malaver, M. (2013) *Black Holes, Wormholes and Dark Energy Stars in General Relativity..* Lambert Academic Publishing, Berlin.
- Malaver, M, Esculpi M, Govender, M. (2019) New Models of Dark Energy Stars with Charge Distributions. *International*

Journal of Astrophysics and Space Science, 7(2): 27-32.

Malaver M, Kasmaei HD (2020) Analytical Models of Dark Energy Stars with Quadratic Equation of State. *Applied Physics* 3: 1-14.

Manjonjo, A.M., Maharaj, S.D., Mooppanar, S. (2017). Conformal vectors and stellar models. *Eur. Phys. J.Plus* 132: 62

Morris, M.S, Thorne K.S. (1988). Wormholes in spacetime and their use for interstellar travel: A tool for teaching general relativity. *Am J Phys* 56: 395-412.

Oppenheimer J.R, Volkoff, G. (1939). On Massive Neutron Cores. *Phys Rev* 55: 374-381.

Rahaman, F., Jamil, M., Sharma, R., Chakraborty, K. (2010). A class of solutions for anisotropic stars admitting conformal motion. *Astrophys. Space. Sci.* 330: 249

Rocha, L. (2023). The masses of neutron stars. PhD thesis. Universidade de São Paulo. Instituto de Astronomia, Geofísica e Ciências Atmosféricas. Departamento de Astronomia. São Paulo, Brasil.

Schwarzschild, K. (1916). On the gravitational field of a sphere of incompressible fluid according to Einstein's theory. *Math Phys Tech.* pp: 424-434.

Sushkov, S. (2005). Wormholes supported by a phantom energy. *Phys Rev D* 71: 043520

Tolman, R.C. (1939). Static Solutions of Einstein's Field Equations for Spheres of Fluid. *Phys Rev* 55: 364-373.

Visser, M. (1995). *Lorentzian wormholes: From Einstein to Hawking*. AIP Press, New York, USA

Weyl, H. (1918). Reine Infinitesimalgeometrie. *Mathematische Zeitschrift*. 2(3): 384